


Coupling impedance of a PEC angular strip in a vacuum pipe

Dario Assante¹  | Gaetano Panariello² | Fulvio Schettino² | Luigi Verolino³

¹Faculty of Engineering, International Telematic University Uninettuno, Italy

²DIEI (Department of Electrical and Information Engineering “Maurizio Scarano”), University of Cassino and Southern Lazio, Cassino, Italy

³Department of Electrical Engineering and Information Technology, University of Naples “Federico II”, Italy

Correspondence

Dario Assante, Faculty of Engineering, International Telematic University Uninettuno, Italy.
Email: d.assante@uninettuno.it

Abstract

This study deals with the evaluation of the longitudinal and transverse coupling impedance of a charge travelling in a drift tube with a perfectly electric conductive angular strip. The problem is formulated in the particle frame as dual series equations, and efficiently solved through the representation of the unknown in terms of Neumann series. Then, the electric parameters are obtained in the pipe frame through the Lorentz transforms. The presented solution can be adopted as the general methodology in case of angular discontinuities in particle accelerators.

1 | INTRODUCTION

Modern particle accelerators require an even higher primary beam energy, in order to investigate unexplored mass regions and to search for the very rare events that would be associated with new particles. This requires even higher dimensions, more powerful magnets and better control systems [1–4].

One critical aspect in the design and control of particle accelerators is the beam instability. This is caused by the interaction between the particle beam and the surrounding structure that is the electromagnetic interaction between the beam and the currents induced on the inner walls of the particle accelerator. This can lead to phenomena such as the frequency shift (change of the betatron or synchrotron frequency), the increase of a small initial disturbance, the bunch instability, or a change of the particle distribution, e.g. bunch lengthening [5–8]. The shape of the different elements constituting the particle accelerator affects the kind of disturbance that can be produced on the particle beam, so their design is essential to ensure the proper performance of the machine [9].

The synthetic design parameter commonly adopted in literature to take into account the effect of a structure on a travelling particle is the coupling impedance [10–12]. This parameter is proportional to the energy lost by the travelling charge due to the interaction with the specific surrounding

structure, or equivalently to the energy to be spent to keep the charge speed at constant nevertheless the surrounding structure. For structures invariant along the charge travelling direction, *per unit length* coupling impedance has to be introduced [11], whose longitudinal and transverse components can be defined as

$$Z_{\parallel}(r, \varphi, k) = -\frac{1}{q} \frac{1}{L} \int_{-L/2}^{L/2} E_z(r, \varphi, z, \omega) e^{jkz/\beta} dz \quad (1a)$$

$$Z_{\perp}(r, \varphi, k) = \frac{1}{k} \nabla_{\perp} Z_{\parallel}(r, \varphi, k) \quad (1b)$$

L being a unitary length, $E_z(r, \varphi, z, \omega)$ the z -component of the electric field in the frequency domain, k the wavenumber, and the charge q is moving at constant velocity $v = \beta c$ along the z axis. The second equation in Equation (1) is known as the Panofski-Wenzel theorem [13].

For complex geometries, numerical tools are adopted to compute the coupling impedance, leveraging on the powerful computing resources that are currently available. Although such a methodology allows getting results in a reasonably short time; for very complex structures, it often does not allow to fully appreciate the dependence of the quantities of interest as a function of the parameters of the problem. On the other

This is an open access article under the terms of the Creative Commons Attribution-NonCommercial-NoDerivs License, which permits use and distribution in any medium, provided the original work is properly cited, the use is non-commercial and no modifications or adaptations are made.

© 2021 The Authors. *IET Microwaves, Antennas & Propagation* published by John Wiley & Sons Ltd on behalf of The Institution of Engineering and Technology.

hand, analytical or semi-analytical methods, although suitable for more canonical geometries, still play a valuable role in this field allowing a better understanding of the physics of some phenomena [14, 15]. Modal analyses are often adopted for closed structures [16], diffractive methods for high-frequency solutions and integral formulations for open geometries or in presence of edges [16–19]. Validation methods are based on the measurement of the coupling impedance using a wire as a source current instead of a travelling charge [20–22].

Most of the studies in the literature concern axial-symmetrical geometries, which also represent most of the existing geometries. In fact, the axial symmetry avoids that the electromagnetic interaction between the structure and the beam tends to deviate the latter from the axis. However, there are also some structures without axial symmetry in particle accelerators. In the present study, we consider the problem of a travelling particle in a pipe in which there is an angular strip, as illustrated in Figure 1. Although the angular strip is in axis with the pipe, its limited angular width creates an asymmetry in the structure. The method used can be easily generalised to other problems of non-axial-symmetrical structures.

Being the structure that is ideally indefinite along the axis of the cylindrical pipe, for such a problem, an electrostatic model can be adopted in the particle frame. The problem is formulated in terms of dual series equations (DSE), as a result of the transformation of the singular integral equation (IE) to the domain of discrete Fourier transform. DSEs are then reduced to the resolution of a linear system. Once the electromagnetic quantities are computed, their values in the angular strip frame can be obtained by means of Lorentz transforms.

In order to distinguish the spatial and electromagnetic quantities, we adopt the primed notation in the particle frame (e.g. z') and the unprimed notation in the pipe frame (e.g. z). Additionally, we use the apex/subscript q to refer to the particle quantities, p to the pipe and s to the angular strip.

2 | FORMULATION OF THE PROBLEM

Let us consider the geometry shown in Figure 1: a perfectly conducting angular strip $\mathbb{S}_s = \{r = a, |\varphi| \leq \varphi_a, z\}$ at distance a from the axis and covering an angular sector of $2\varphi_a$, inside a cylinder $\mathbb{S}_p = \{r = b, \varphi, z\}$ at distance $b > a$ from the axis. A travelling charge q moves parallel to the angular strip's axis,

placed at (r_q, φ_q) , at constant speed $v = \beta c$, being c the speed of light in free space.

It is useful to introduce a temporal and a spatial Fourier transform

$$F(\omega) = \int_{-\infty}^{+\infty} f(t)e^{-j\omega t} dt \quad f(t) = \frac{1}{2\pi} \int_{-\infty}^{+\infty} F(\omega)e^{j\omega t} d\omega \quad (2)$$

$$\tilde{f}(\omega) = \frac{1}{2\pi} \int_{-\infty}^{+\infty} f(z)e^{j\omega z} dz \quad f(z) = \int_{-\infty}^{+\infty} \tilde{f}(\omega)e^{-j\omega z} d\omega \quad (3)$$

For clarity of notation, we specify that we use the notation $f(z, t)$ in time and space domain, $F(z, \omega)$ when introducing a time Fourier transform and $\tilde{f}(\omega, t)$ when introducing a spatial Fourier transform.

It is convenient to formulate the problem in the particle frame since, as anticipated in the previous section, an electrostatic formulation can be adopted. The expression of the electric field due to a charge in a perfectly conductive cylindrical pipe can be expressed, as shown in the appendix, as

$$e'_{r,qp} = -q \sum_{m=-\infty}^{+\infty} e^{jm(\varphi' - \varphi_q)} \int_{-\infty}^{+\infty} \frac{\partial G_m^{qp}}{\partial r'}(r', r_q, \omega) e^{-j\omega z'} d\omega \quad (4)$$

$$e'_{\varphi,qp} = -\frac{j2q}{r'} \sum_{m=-\infty}^{+\infty} m e^{jm(\varphi' - \varphi_q)} \int_{-\infty}^{+\infty} G_m^{qp}(r', r_q, \omega) e^{-j\omega z'} d\omega \quad (5)$$

$$e'_{z,qp} = jq \sum_{m=-\infty}^{+\infty} e^{jm(\varphi' - \varphi_q)} \int_{-\infty}^{+\infty} \omega G_m^{qp}(r', r_q, \omega) e^{-j\omega z'} d\omega \quad (6)$$

where

$$G_m^{qp}(r', r_q, \omega) = \frac{1}{4\pi^2 \epsilon_0} \cdot \begin{cases} K_m(\omega r') I_m(\omega r_q) - \frac{I_m(\omega r_q)}{I_m(\omega b)} K_m(\omega b) I_m(\omega r'); & r' \geq r_q \\ K_m(\omega r_q) I_m(\omega r') - \frac{I_m(\omega r_q)}{I_m(\omega b)} K_m(\omega b) I_m(\omega r'); & r' \leq r_q \end{cases} \quad (7)$$

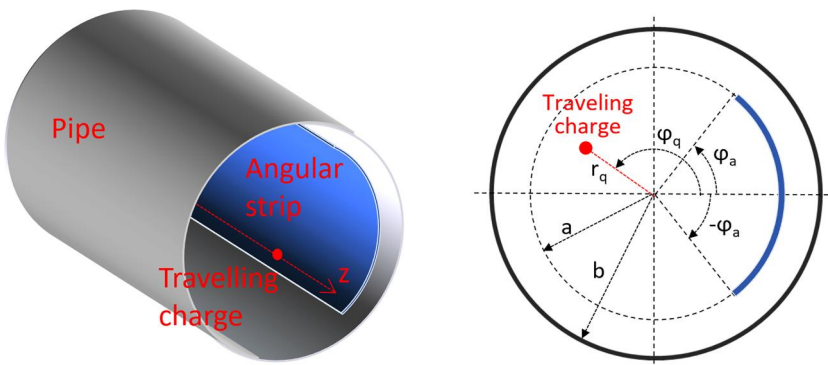


FIGURE 1 Geometry of the problem

A charge density $\sigma'_s(r' = a, \varphi', z')$ is induced on the angular strip. The components of the electric field generated by such charge density can be expressed, in analogy with the previous expressions, as

$$e'_{r,s} = -2\pi a \sum_{m=-\infty}^{+\infty} e^{jm\varphi'} \cdot \int_{-\varphi_a}^{+\varphi_a} \int_{-\infty}^{+\infty} \tilde{\sigma}_s(\varphi'_0, \omega) \frac{\partial G_m^{qp}}{\partial r'}(r', a, \omega) e^{-j\omega z'} e^{-jm\varphi'_0} d\omega d\varphi'_0 \quad (8)$$

$$e'_{\varphi,s} = -\frac{j4\pi a}{r'} \sum_{m=-\infty}^{+\infty} m e^{jm\varphi'} \cdot \int_{-\varphi_a}^{+\varphi_a} \int_{-\infty}^{+\infty} \tilde{\sigma}_s(\varphi'_0, \omega) G_m^{qp}(r', a, \omega) e^{-j\omega z'} e^{-jm\varphi'_0} d\omega d\varphi'_0 \quad (9)$$

$$e'_{z,s} = 2\pi a j \sum_{m=-\infty}^{+\infty} e^{jm\varphi'} \cdot \int_{-\varphi_a}^{+\varphi_a} \int_{-\infty}^{+\infty} \tilde{\sigma}_s(\varphi'_0, \omega) \omega G_m^{qp}(r', a, \omega) e^{-j\omega z'} e^{-jm\varphi'_0} d\omega d\varphi'_0 \quad (10)$$

being $\tilde{\sigma}_s(\varphi'_0, \omega)$ the spatial transform of $\sigma_s(\varphi'_0, z'_0)$ according to Equation (3). It is worth noting that the above expressions do not represent the electric field of an angular strip in the free space, but of an angular strip in the pipe. This is evident by observing that the fields $e'_{\varphi,s}$ and $e'_{z,s}$ vanish on the pipe by construction, since $G_m^{qp}(b, a, \omega) = 0$.

Being the surfaces that are perfectly conducting, the boundary condition to be verified is the tangential components of the electric field that vanish on them, namely

$$e'_{z,s}(r' = a, \varphi', z') + e'_{z,qp}(r' = a, \varphi', z') = 0 \quad (11)$$

$$e'_{\varphi,s}(r' = a, \varphi', z') + e'_{\varphi,qp}(r' = a, \varphi', z') = 0 \quad (12)$$

for every $(\varphi', z') \in S_s$.

Considering the expressions Equations (10) and (6) and performing an inverse Fourier transform along z, Equation (11) leads to

$$\sum_{m=-\infty}^{+\infty} e^{jm\varphi'} G_m^{qp}(a, a, \omega) \int_{-\varphi_a}^{+\varphi_a} \tilde{\sigma}_s(\varphi'_0, \omega) e^{-jm\varphi'_0} d\varphi'_0 = -\frac{q}{2\pi a} \sum_{m=-\infty}^{+\infty} e^{jm(\varphi'-\varphi_q)} G_m^{qp}(a, r_q, \omega) \quad (13)$$

for $|\varphi'| \leq \varphi_a$.

Considering the expressions Equations (9) and (5) and performing an inverse Fourier transform again along z, Equation (12) leads to

$$\sum_{m=-\infty}^{+\infty} m e^{jm\varphi'} \int_{-\varphi_a}^{+\varphi_a} \tilde{\sigma}_s(\varphi'_0, \omega) G_m^{qp}(a, a, \omega) e^{-jm\varphi'_0} d\varphi'_0 = -\frac{q}{2\pi a} \sum_{m=-\infty}^{+\infty} m e^{jm(\varphi'-\varphi_q)} G_m^{qp}(a, r_q, \omega) \quad (14)$$

It is trivial to observe that Equation (14) can be obtained by deriving Equation (13) with respect to φ' . Therefore, if Equation (13) is satisfied for every φ' , then Equation (14) is verified as well.

In order to ensure the uniqueness of the solution, it is also necessary to impose another condition in the complementary domain, that is

$$\tilde{\sigma}_s(\varphi'_0, \omega) = 0 \quad \forall |\varphi'_0| > \varphi_a \quad (15)$$

Equations (13) and (15) constitute a system of dual series equations (DSE). To efficiently solve the problem, it is possible to represent the unknown in terms of Neumann series [23]:

$$\tilde{\sigma}'_s(\varphi', \omega) = \begin{cases} -\frac{q}{2\pi^2 a \varphi_a} \sum_{n=0}^{\infty} j^n \tilde{\sigma}_n(\omega) \frac{T_n(\varphi'/\varphi_a)}{\sqrt{1 - (\varphi'/\varphi_a)^2}}, & |\varphi| \leq \varphi_a \\ 0, & |\varphi| > \varphi_a \end{cases} \quad (16)$$

where $T_n(\cdot)$ is the Chebychev polynomial of order n [24]. With such a normalisation, dimensionless expansion coefficients are obtained in the transformed domain.

The chosen representation takes origin from the more generical Neumann series, particularised for this problem [23]. It automatically matches the right edge behaviour, thus regularising the method and reducing the computational effort for the numerical evaluation of the solution.

In addition, the chosen current density representation already vanishes outside the angular strip. Then, by taking advantage of the relevant integral [23].

$$\int_{-\varphi_a}^{+\varphi_a} \frac{T_n(\varphi'/\varphi_a)}{\sqrt{1 - (\varphi'/\varphi_a)^2}} e^{jm\varphi'} d\varphi' = \varphi_a \pi j^n J_n(m\varphi_a) \quad (17)$$

and by substituting the representation Equation (16) into Equation (13), it is found that

$$\sum_{n=0}^{\infty} \tilde{\sigma}_n(\omega) \sum_{m=-\infty}^{+\infty} e^{jm\varphi'} J_n(m\varphi_a) G_m^{qp}(a, a, \omega) = \sum_{m=-\infty}^{+\infty} e^{jm(\varphi'-\varphi_q)} G_m^{qp}(a, r_q, \omega) \quad (18)$$

By projecting Equation (18) on the same representation basis and integrating over ϕ' , in the end it can be found

$$\begin{aligned} \sum_{n=0}^{\infty} \tilde{\sigma}_n(\omega) \sum_{m=-\infty}^{+\infty} J_n(m\varphi_a) J_r(m\varphi_a) G_m^{qp}(a, a, \omega) &= \\ = \sum_{m=-\infty}^{+\infty} J_r(m\varphi_a) G_m^{qp}(a, r_q, \omega) e^{-jm\varphi_q} &\quad (19) \end{aligned}$$

In such a way, the solution of the DSE Equations (13)–(15) is converted into a linear system in the form

$$\mathbf{A}\tilde{\sigma} = \mathbf{b} \quad (20)$$

whose solution allows to evaluate the expansion coefficients $\tilde{\sigma}_n$. The terms of the symmetric matrix \mathbf{A} can be expressed with some manipulations as

$$\begin{aligned} A_{nr} &= \\ &= \begin{cases} \delta_{0n} \delta_{0r} G_0^{qp}(a, a, \omega) + \\ + 2 \sum_{m=1}^{+\infty} J_n(m\varphi_a) J_r(m\varphi_a) G_m^{qp}(a, a, \omega), & n+r \text{ even} \\ 0, & n+r \text{ odd} \end{cases} \quad (21) \end{aligned}$$

δ_{nr} is the Kronecker symbol. The elements of the known term are

$$\begin{aligned} b_r &= \\ &= \begin{cases} \delta_{0r} G_0^{qp}(a, r_q, \omega) + \\ + 2 \sum_{m=1}^{+\infty} \cos(m\varphi_q) J_r(m\varphi_a) G_m^{qp}(a, r_q, \omega) & r \text{ even} \\ -2j \sum_{m=1}^{+\infty} \sin(m\varphi_q) J_r(m\varphi_a) G_m^{qp}(a, r_q, \omega) & r \text{ odd} \end{cases} \quad (22) \end{aligned}$$

These results allow us to make several considerations about the solution. The fact that the terms A_{nr} are null when $n+r$ is odd implies that the matrix \mathbf{A} can be split into two submatrices, allowing the unknown coefficients even and odd to be calculated separately. Moreover, since $\varphi_q = 0$ the odd coefficients of b_r are zero; similarly, the odd coefficients of σ_n are also zero. Therefore, we find what is expected by the symmetry of the problem in the formulation, i.e. when the particle is on the axis of symmetry of the angular strip, the induced current on the strip is an even function. Finally, since all the terms of A_{nr} are real, while the b_r are real for r even and imaginary for r odd, the coefficients σ_n are also real for n even and imaginary for n odd. Given the equation (16), this implies that the expression of the induced current is always real.

2.1 | Computational enhancement

Although equation (20) formally solves the problem, unfortunately equation (21) has a very slow convergence that affects the numerical computation.

For high values of m , the following approximation is valid for $n+r$ even [24]

$$\begin{aligned} J_n(m\varphi_a) J_r(m\varphi_a) G_m^{qp}(a, a, \omega) &\simeq \\ \simeq \frac{(-1)^{\frac{n+r}{2}}}{8\pi^3 \varphi_a \epsilon_0} \left(1 - \left(\frac{a}{b}\right)^{2m} \right) \frac{1 + \sin(2m\varphi_a)}{m^2} &\quad (23) \end{aligned}$$

and in general

$$\begin{aligned} J_r(m\varphi_a) G_m^{qp}(a, r_q, \omega) &\simeq \frac{1}{2^{5/2} \pi^{5/2} \varphi_a^{1/2} \epsilon_0} \\ \cdot \left(\frac{r_q^m}{a^m} - \frac{r_q^m a^m}{b^{2m}} \right) \frac{\cos(m\varphi_a - r\pi/2 - \pi/4)}{m^{3/2}} &\quad (24) \end{aligned}$$

Additionally, it is known that

$$\sum_{m=1}^{\infty} x^m \frac{\sin(my)}{m^s} = \frac{j}{2} (Li_s(xe^{-jy}) - Li_s(xe^{jy})) \quad (25)$$

$$\sum_{m=1}^{\infty} x^m \frac{\cos(my)}{m^s} = \frac{1}{2} (Li_s(xe^{-jy}) + Li_s(xe^{jy})) \quad (26)$$

$Li_s(\cdot)$ being the polylogarithmic function of index s . Note that Equations (25) and (26) are the sum of real function, so their sums are real even if expressed as the sum of complex functions [26].

Therefore, Equation (20) can be rewritten as

$$(\mathbf{A}^0 + \mathbf{A}^\infty)\tilde{\sigma} = \mathbf{b}^0 + \mathbf{b}^\infty \quad (27)$$

where, remembering that the matrix must be calculated only for $n+r$ even

$$\begin{aligned} A_{nr}^0 &= \delta_{0n} \delta_{0r} G_0^{qp}(a, a, \omega) + \\ &+ 2 \sum_{m=1}^{+\infty} \left[J_n(m\varphi_a) J_r(m\varphi_a) G_m^{qp}(a, a, \omega) + \right. \\ &\left. - \frac{(-1)^{\frac{n+r}{2}}}{8\pi^3 \varphi_a \epsilon_0} \left(1 - \left(\frac{a}{b}\right)^{2m} \right) \frac{1 + \sin(2m\varphi_a)}{m^2} \right] \quad (28) \end{aligned}$$

$$\begin{aligned} A_{nr}^\infty &= \frac{(-1)^{\frac{n+r}{2}}}{8\pi^3 \varphi_a \epsilon_0} \left[\frac{\pi^2}{6} - Li_2\left(\frac{a^2}{b^2}\right) + \right. \\ &+ \frac{j}{2} (Li_2(e^{-j2\varphi_a}) - Li_2(e^{j2\varphi_a})) + \\ &\left. - \frac{j}{2} \left(Li_2\left(\frac{a^2}{b^2} e^{-j2\varphi_a}\right) - Li_2\left(\frac{a^2}{b^2} e^{j2\varphi_a}\right) \right) \right] \quad (29) \end{aligned}$$

and for r even

$$\begin{aligned}
 b_r^0 &= \delta_{0r} G_0^{qp}(a, r_q, \omega) + \\
 &+ 2 \sum_{m=1}^{+\infty} \cos(m\varphi_q) \left[J_r(m\varphi_a) G_m^{qp}(a, r_q, \omega) + \right. \\
 &\left. - \frac{(-1)^{r/2}}{2^{5/2} \pi^{5/2} \varphi_a^{1/2} \epsilon_0} \left(\frac{r_q^m}{a^m} - \frac{r_q^m a^m}{b^{2m}} \right) \frac{\cos(m\varphi_a - \pi/4)}{m^{3/2}} \right] \\
 b_r^\infty &= \frac{(-1)^{r/2}}{16 \pi^{5/2} \varphi_a^{1/2} \epsilon_0} \\
 &\cdot \left[(1+j) \left[Li_{3/2} \left(\frac{r_q}{a} e^{-j(\varphi_a - \varphi_q)} \right) - Li_{3/2} \left(\frac{r_q a}{b^2} e^{-j(\varphi_a - \varphi_q)} \right) \right] + \right. \\
 &+ Li_{3/2} \left(\frac{r_q}{a} e^{-j(\varphi_a + \varphi_q)} \right) - Li_{3/2} \left(\frac{r_q a}{b^2} e^{-j(\varphi_a + \varphi_q)} \right) \left. \right] + \\
 &+ (1-j) \left[Li_{3/2} \left(\frac{r_q}{a} e^{j(\varphi_a - \varphi_q)} \right) - Li_{3/2} \left(\frac{r_q a}{b^2} e^{j(\varphi_a - \varphi_q)} \right) \right] + \\
 &+ Li_{3/2} \left(\frac{r_q}{a} e^{j(\varphi_a + \varphi_q)} \right) - Li_{3/2} \left(\frac{r_q a}{b^2} e^{j(\varphi_a + \varphi_q)} \right) \left. \right] \quad (30)
 \end{aligned}$$

and for r odd

$$\begin{aligned}
 b_r^0 &= -2j \sum_{m=1}^{+\infty} \sin(m\varphi_q) \left[J_r(m\varphi_a) G_m^{qp}(a, r_q, \omega) + \right. \\
 &\left. - \frac{(-1)^{(r-1)/2}}{2^{5/2} \pi^{5/2} \varphi_a^{1/2} \epsilon_0} \left(\frac{r_q^m}{a^m} - \frac{r_q^m a^m}{b^{2m}} \right) \frac{\cos(m\varphi_a - \pi/4)}{m^{3/2}} \right] \\
 b_r^\infty &= \frac{(-1)^{(r-1)/2}}{16 \pi^{5/2} \varphi_a^{1/2} \epsilon_0} \\
 &\cdot \left[(-1-j) \left[Li_{3/2} \left(\frac{r_q}{a} e^{-j(\varphi_a - \varphi_q)} \right) - Li_{3/2} \left(\frac{r_q a}{b^2} e^{-j(\varphi_a - \varphi_q)} \right) \right] + \right. \\
 &- Li_{3/2} \left(\frac{r_q}{a} e^{-j(\varphi_a + \varphi_q)} \right) + Li_{3/2} \left(\frac{r_q a}{b^2} e^{-j(\varphi_a + \varphi_q)} \right) \left. \right] + \\
 &+ (1-j) \left[Li_{3/2} \left(\frac{r_q}{a} e^{j(\varphi_a - \varphi_q)} \right) - Li_{3/2} \left(\frac{r_q a}{b^2} e^{j(\varphi_a - \varphi_q)} \right) \right] + \\
 &- Li_{3/2} \left(\frac{r_q}{a} e^{j(\varphi_a + \varphi_q)} \right) + Li_{3/2} \left(\frac{r_q a}{b^2} e^{j(\varphi_a + \varphi_q)} \right) \left. \right] \quad (31)
 \end{aligned}$$

It is worth noting that Equations (29), (31) and (33) do not depend by the parameter ω . On one hand, it means that they can be computed just once even if it is necessary to perform a sweep over ω , thus further reducing the computational effort.

On the other hand, it means that the quality of the approximation depends on such a parameter that is the smaller ω is, the better is the approximation. This will be discussed again in Section 4.

3 | COUPLING IMPEDANCE

Once the induced current density on the angular strip is computed, in order to evaluate the coupling impedance, it is possible to compute the electromagnetic field and so the coupling impedance.

According to the previous decomposition, the z-component of the total electric field is the sum of the quantities $E_{z,qp}$ and $E_{z,s}$. However, in order to calculate the coupling impedance, it is necessary to subtract from the total field the contribution of the field produced by the charge itself.

Therefore, the expression of the electric field to be calculated for the evaluation of the coupling impedance can be expressed as

$$E_z(r, \varphi, z, \omega) = E_{z,p}(r, \varphi, z, \omega) + E_{z,s}(r, \varphi, z, \omega) \quad (34)$$

In the particle frame, the field $E'_{z,p}$ has the same expression of using Equation (6) instead the kernel Equation (56), while the field $E'_{z,s}$ is expressed according to Equation (10).

At first, it is necessary to perform a change of reference, in order to express the electric field in the pipe frame. This can be easily performed by the Lorentz transforms [27]. Considering that the charge travels parallel to the z-axis, the transforms areas follows:

$$e'_z = e_z, \quad d' = q\gamma, \quad \sigma' = \sigma\gamma, \quad r' = r, \quad \varphi' = \varphi, \quad z' = \gamma(z - vt). \quad (35)$$

where $\gamma = 1/\sqrt{1 - \beta^2}$ is the Lorentz factor.

By applying the Lorentz transform to the field $e'_{z,p}$ and then Equation (2) in the pipe frame in the frequency domain, it is found

$$E_{z,p} = \frac{j2\pi qk}{\beta} \sum_{m=-\infty}^{+\infty} e^{jm(\varphi - \varphi_q)} G_m^p(r, r_q, \kappa) e^{-jkz/\beta} \quad (36)$$

being $k = \omega/c$ and $\kappa = k/\beta\gamma$.

With similar operations, it can be found that

$$\begin{aligned}
 E_{z,s} &= -\frac{jq\pi k}{\beta} \sum_{m=-\infty}^{+\infty} e^{jm\varphi} G_m^{qp}(r, a, \kappa) \cdot \\
 &\cdot \sum_{n=0}^{\infty} \tilde{\sigma}_n(\kappa) J_n(m\varphi_a) e^{-jkz/\beta}
 \end{aligned} \quad (37)$$

Therefore, considering the definition Equation (1) and the electric fields Equations (36) and (37), the longitudinal coupling impedance can be finally expressed as

$$\begin{aligned}
Z_{\parallel,\varphi}(r, \varphi, k) &= \\
&= -\frac{j\pi k}{\beta} \sum_{m=-\infty}^{+\infty} e^{jm\varphi} \left(2e^{-jm\varphi_a} G_m^p(r, r_q, \kappa) + \right. \\
&\quad \left. - G_m^{qp}(r, a, \kappa) \sum_{n=0}^{\infty} \tilde{\sigma}_n(\kappa) J_n(m\varphi_a) \right) \quad (38)
\end{aligned}$$

By applying the Panofski-Wenzel theorem Equation (1b), it is also possible to evaluate the two components of the transverse impedance

$$\begin{aligned}
Z_{\perp,r}(r, \varphi, k) &= \\
&= -\frac{j2\pi}{\beta} \sum_{m=-\infty}^{+\infty} e^{jm\varphi} \left(e^{-jm\varphi_a} \frac{\partial G_m^p}{\partial r}(r, r_q, \kappa) + \right. \\
&\quad \left. - \frac{\partial G_m^{qp}}{\partial r}(r, a, \kappa) \sum_{n=0}^{\infty} \tilde{\sigma}_n(\kappa) J_n(m\varphi_a) \right) \quad (39)
\end{aligned}$$

$$\begin{aligned}
Z_{\perp,\varphi}(r, \varphi, k) &= \\
&= \frac{2\pi}{r\beta} \sum_{m=-\infty}^{+\infty} m e^{jm\varphi} \left(e^{-jm\varphi_a} G_m^p(r, r_q, \kappa) + \right. \\
&\quad \left. - G_m^{qp}(r, a, \kappa) \sum_{n=0}^{\infty} \tilde{\sigma}_n(\kappa) J_n(m\varphi_a) \right) \quad (40)
\end{aligned}$$

3.1 | Special case: particle on the axis

The previous expressions of the longitudinal and transverse impedance have general validity. However, they are usually computed under particular conditions.

Under normal operating conditions, the travelling charge moves in a particle accelerator along the pipe axis. So, the most important and also generally considered condition for the analyses is $r_q = 0$.

Additionally, the coupling impedance itself is evaluated along the pipe axis, i.e. $r = 0$.

In such conditions, it has to be considered that

$$G_m^p(0, 0, \kappa) = \begin{cases} -\frac{1}{4\pi^2\epsilon_0} \frac{K_0(b\kappa)}{I_0(b\kappa)}, & m = 0 \\ 0, & m > 0 \end{cases} \quad (41)$$

$$G_m^{qp}(0, a, \kappa) = \begin{cases} \frac{1}{4\pi^2\epsilon_0} \left(K_0(a\kappa) - \frac{I_0(a\kappa)}{I_0(b\kappa)} K_0(b\kappa) \right), & m = 0 \\ 0, & m > 0 \end{cases} \quad (42)$$

Then Equations (38), (39) and (40) reduce to

$$Z_{\parallel}(0, k) = -\frac{j2\pi k}{\beta} (G_0^p(0, 0, \kappa) - \tilde{\sigma}_0(\kappa) G_0^{qp}(0, a, \kappa)) \quad (43)$$

$$\begin{aligned}
Z_{\perp,r}(0, \varphi, k) &= \frac{j\kappa}{2\pi\epsilon_0\beta} e^{j\varphi} \cdot \\
&\quad \cdot \left(K_1(\kappa a) - \frac{I_1(\kappa a)}{I_1(\kappa b)} K_1(\kappa b) \right) \sum_{n=0}^{\infty} \tilde{\sigma}_n(\kappa) J_n(\varphi_a) \quad (44)
\end{aligned}$$

$$\begin{aligned}
Z_{\perp,\varphi}(0, \varphi, k) &= -\frac{\kappa}{2\pi\epsilon_0\beta} e^{j\varphi} \cdot \\
&\quad \cdot \left(K_1(\kappa a) - \frac{I_1(\kappa a)}{I_1(\kappa b)} K_1(\kappa b) \right) \sum_{n=0}^{\infty} \tilde{\sigma}_n(\kappa) J_n(\varphi_a) \quad (45)
\end{aligned}$$

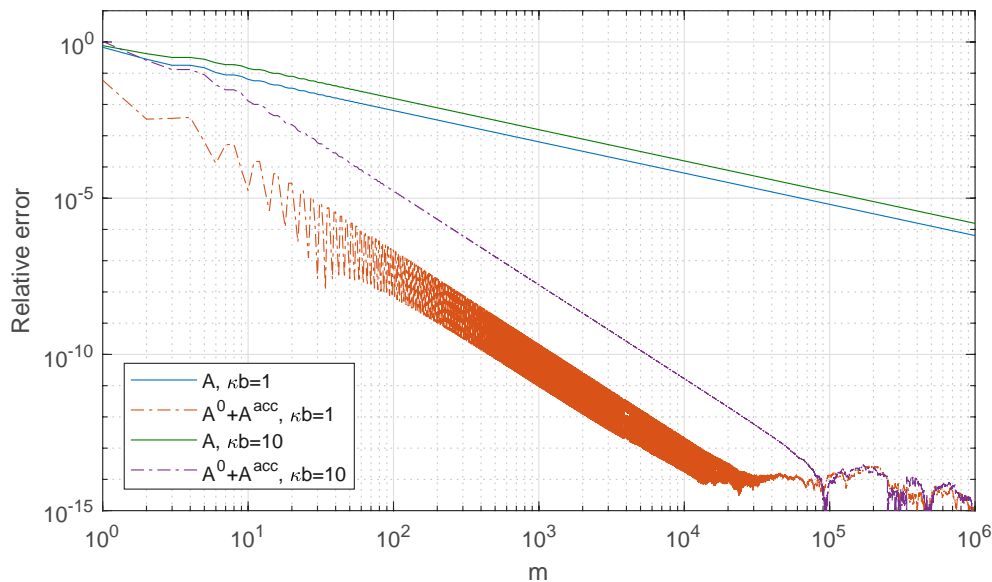


FIGURE 2 Convergence of the term A_{00} with different computational methods. Parameters: $\beta = 0.9$, $b = 10$ cm, $a = 8$ cm, $\varphi_a = 45^\circ$

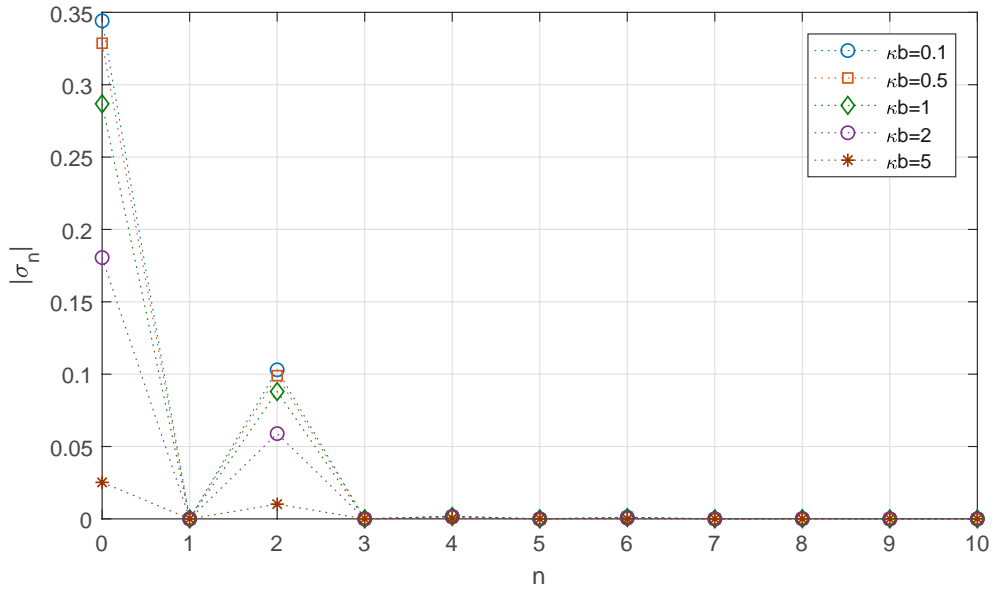


FIGURE 3 Coefficients σ_n for different values of κb . Parameters: $\beta = 0.9, b = 10 \text{ cm}, a = 8 \text{ cm}, \varphi_a = 45^\circ, r_q = 0$

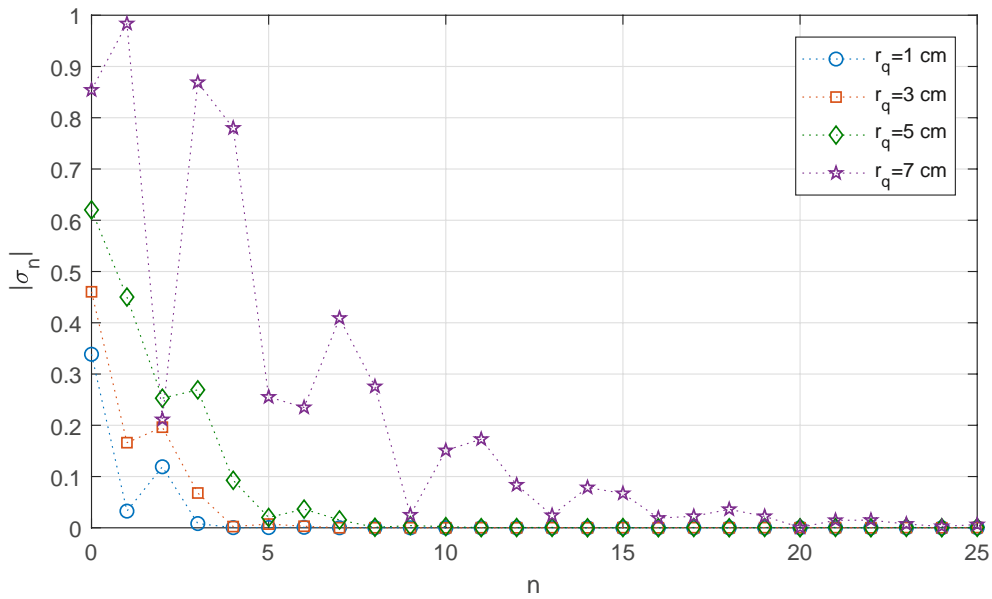


FIGURE 4 Coefficients σ_n for different distances of the particle from the angular strip. Parameters: $\beta = 0.9, b = 10 \text{ cm}, a = 8 \text{ cm}, \varphi_a = 45^\circ, \varphi_q = 30^\circ, \kappa b = 1$

Considering that $\hat{x} = \hat{r} \cos \varphi - \hat{\varphi} \sin \varphi$, the two expressions of the transverse coupling impedance can be combined into one directed along the \hat{x} axis as

$$Z_{\perp,x}(0, \varphi, k) = \frac{j\kappa}{2\pi\epsilon_0\beta} \cdot \left(K_1(\kappa a) - \frac{I_1(\kappa a)}{I_1(\kappa b)} K_1(\kappa b) \right) \sum_{n=0}^{\infty} \tilde{\sigma}_n(\kappa) J_n(\varphi_a) \tag{46}$$

Such a result is coherent with the symmetry of the structure.

4 | NUMERICAL RESULTS

Before showing some calculations of the coupling impedance, it is worth discussing about the efficiency of the proposed method.

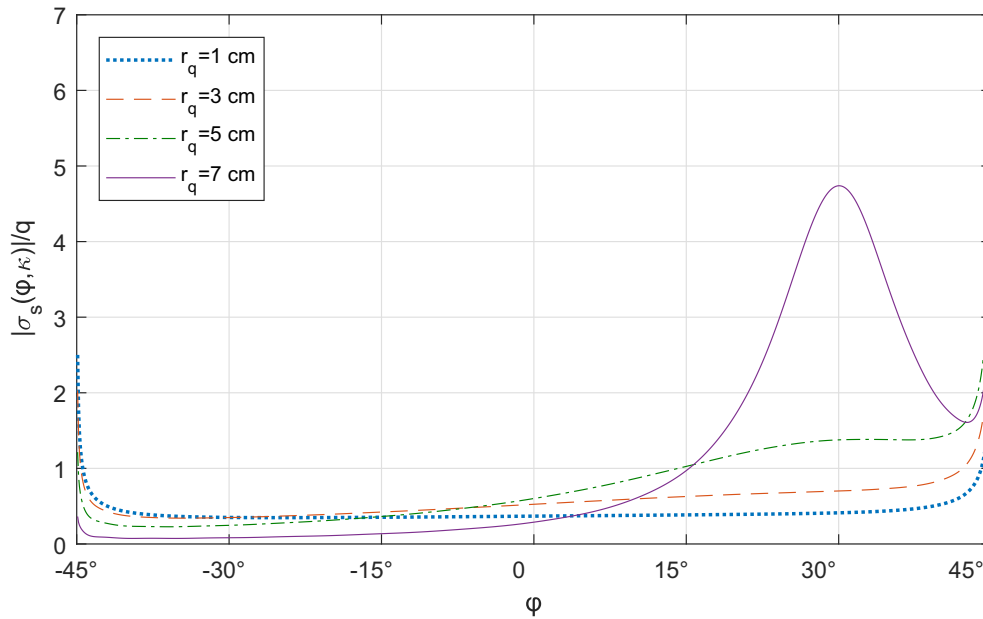


FIGURE 5 Charge density $\tilde{\sigma}'_s(\varphi', \kappa)$ for different distances of the particle from the angular strip. Parameters: $\beta = 0.9$, $b = 10$ cm, $a = 8$ cm, $\varphi_a = 45^\circ$, $\varphi_q = 30^\circ$, $\kappa b = 1$

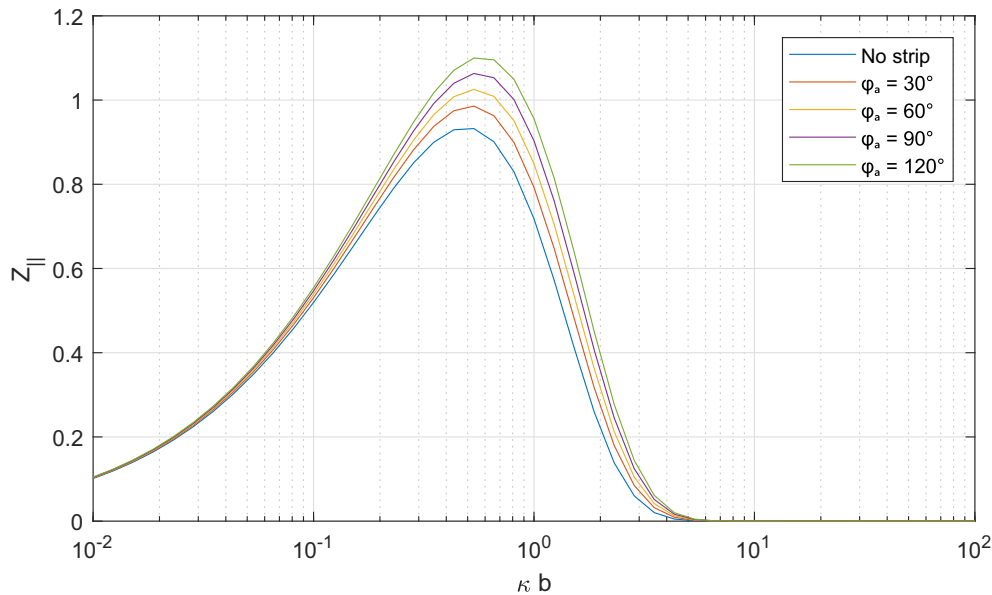


FIGURE 6 Longitudinal coupling impedance for different amplitudes of the strip. Parameters: $\beta = 0.9$, $b = 10$ cm, $a = 8$ cm

First, it is worthy to discuss the advantage of rewriting the problem as in Equation (27). Therefore, as an example, we consider the element $A_{0,0}$ of the system matrix, which is also the most relevant one. We consider a pipe with a radius $b = 10$ cm and an angular strip of radius $a = 8$ cm and semi-amplitude $\varphi_a = 45^\circ$. We compute the partial sums of Equation (21) and the sum of Equations (28) and (29) as the function of m , evaluating the relative error with respect to the asymptotic values computed with 10^9 terms. The results are shown in Figure 2 in the cases of $\kappa b = 1$ and $\kappa b = 10$. To reach

a relative error of 10^{-6} about 1.000.000 terms are required computing the whole series, while less than 1.000 are required analytically subtracting the asymptotic part. Additionally, as expected, the benefit of the approximation slightly decreases as κ increases, still providing an excellent improvement even at higher frequencies.

Then, we discuss about the efficiency of the method and the convergence of the series σ_n . The proposed method turns out to be extremely efficient in the case of greater real interest, that is $r_q = 0$, about 10 coefficients are enough to correctly

reconstruct the current density. This is illustrated in Figure 3 for different values of $b \kappa$. It is worth noting that in such a condition, as expected, the odd coefficients are zero.

The number of coefficients slightly increases as the particle is closer to the angular strip; in Figure 4, the coefficients are shown for different positions of the particle. The effect can be better understood in Figure 5, where the function $\tilde{\sigma}'_s(\varphi', \kappa)$ is shown in the same conditions. It is evident that as the particle approaches the strip, the charge density exhibits a behaviour that tends towards a singularity, which requires more coefficients to be reconstructed. However, even when the particle

is very close to the strip, which is a condition far from reality, the method is found to be very efficient. In these simulations, we have chosen $\varphi_q \neq 0$ to show the appearance of odd coefficients too.

The, we show some calculations of the coupling impedance, in the case of main interest $r_q = 0$ and $r = 0$. According to the considerations of the previous section, all the plots are related to the imaginary part of the coupling impedance, and the real part being null.

In Figures 6 and 7, we choose $\beta = 0.9$, showing the behaviour of the longitudinal and transverse impedance as

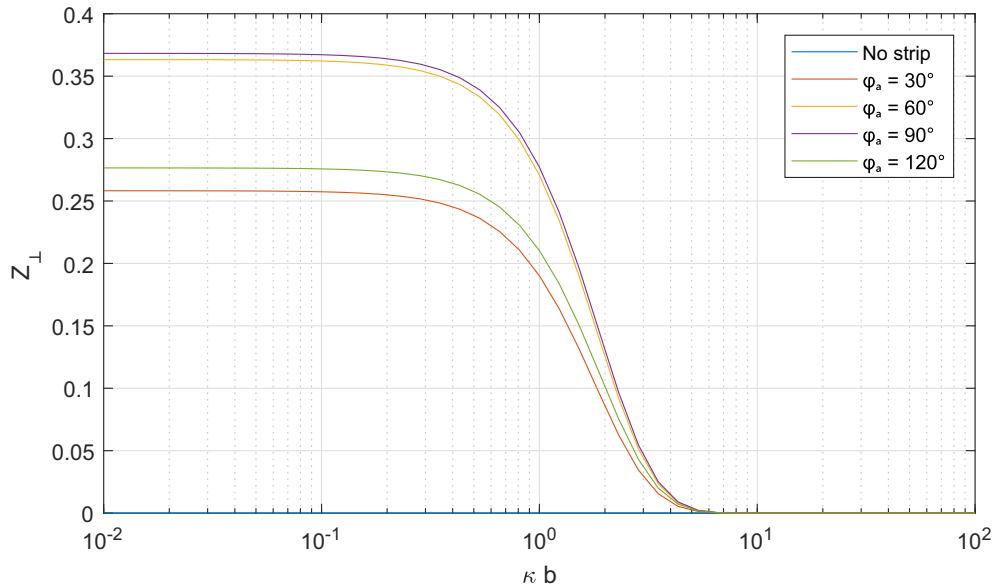


FIGURE 7 Transverse coupling impedance for different amplitudes of the strip. Parameters: $\beta = 0.9$, $b = 10$ cm, $a = 8$ cm

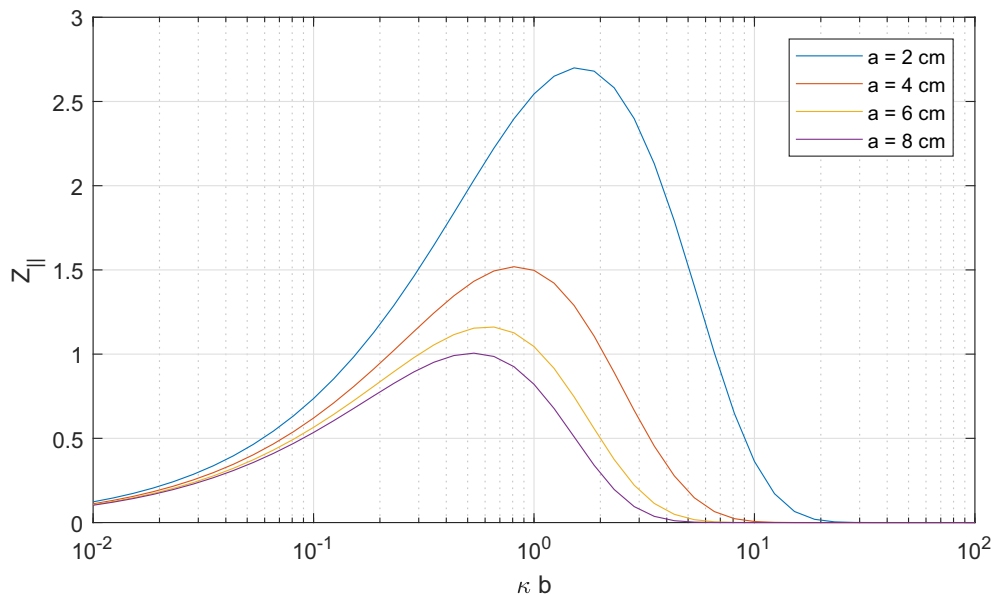


FIGURE 8 Longitudinal coupling impedance for different radii of the strip. Parameters: $\beta = 0.9$, $b = 10$ cm, $\varphi_a = 45^\circ$

function of the strip amplitude. The blue line corresponds to the case $\varphi_a = 0$, that is the pipe in the absence of the angular strip. As the strip's amplitude increases, the longitudinal coupling impedance increases as well. This can be justified considering that an even bigger structure is going to be placed closer to the particle, and reducing the distance between the particle and the surrounding structure increased the electromagnetic interaction and so the longitudinal impedance. The transverse coupling impedance exhibits a different behaviour as function of the strip's

amplitude. When $\varphi_a = 0$, the transverse impedance vanishes due to the angular symmetry. As the amplitude increases, the transverse impedance increases until it reaches its maximum for $\varphi_a = 90^\circ$. Then it decreases, as it has to vanish again for $\varphi_a = 180^\circ$ as the angular symmetry is restored.

In Figures 8 and 9, we consider a strip semi-amplitude $\varphi_a = 30^\circ$, showing the behaviour of the longitudinal and transverse impedance as function of the strip radius. As expected, the impedance significantly increases as the radius

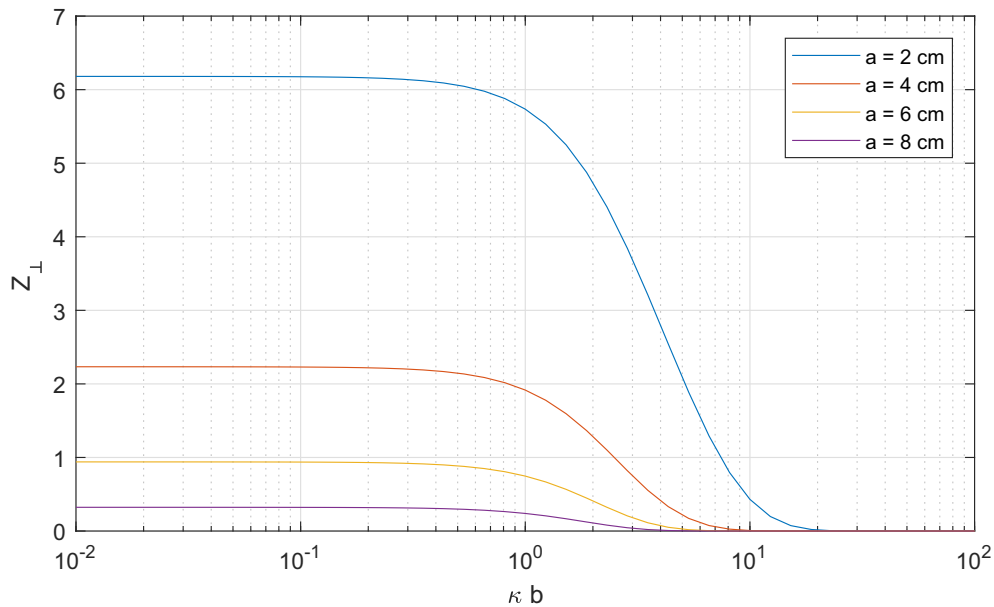


FIGURE 9 Transverse coupling impedance for different radii of the strip. Parameters: $\beta = 0.9$, $b = 10$ cm, $\varphi_a = 45^\circ$

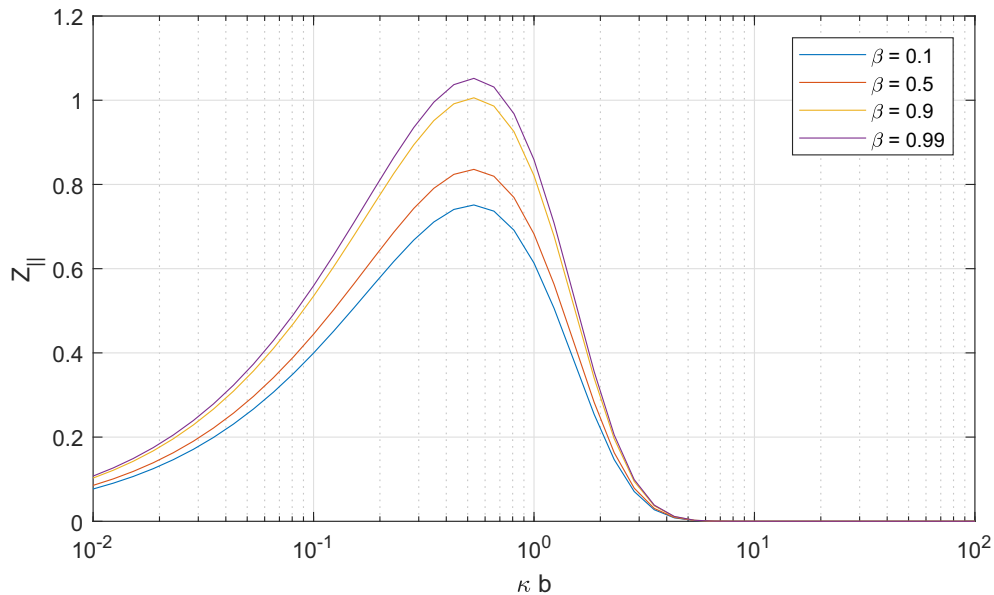


FIGURE 10 Longitudinal coupling impedance for different charge speeds. Parameters: $b = 10$ cm, $a = 8$ cm, $\varphi_a = 45^\circ$

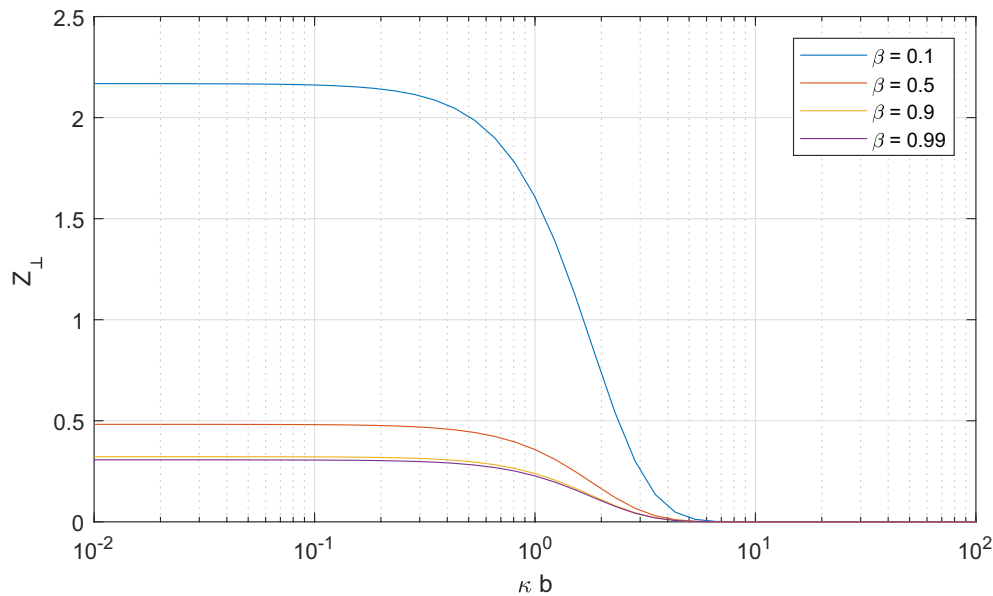


FIGURE 11 Transverse coupling impedance for different charge speeds. Parameters: $b = 10$ cm, $a = 8$ cm, $\varphi_a = 45^\circ$

decreases, the electromagnetic interaction being stronger between the charge and the strip.

Finally, in Figures 10 and 11 we choose $a = 5$ cm and $\varphi_a = 30^\circ$, then performing a sweep on the charge speed. In this case, it is found that the longitudinal coupling impedance increases as the particle speed, while the transverse coupling impedance decreases.

5 | CONCLUSIONS

In this study, a method for the analysis of electromagnetic problems in the presence of non-axial-symmetrical and edge structures has been applied to a canonical problem relevant to accelerator physics: a charge travelling in a pipe with an angular strip inside. Thanks to the proper choice of the representation basis satisfying the edge conditions, the proposed method allows to efficiently and accurately compute the parameters of interest. The method can be easily generalised to different kinds of non-axial-symmetrical geometries.

FUNDING

None.

ORCID

Dario Assante  <https://orcid.org/0000-0001-9333-5034>

REFERENCES

- Wilson, E.J.: An Introduction to Particle Accelerators. Clarendon Press (2001)
- Thomson, M.: Modern Particle Physics. Cambridge University Press (2013)
- Chernyaev, A.P., Varzar, S.M.: Particle accelerators in modern world. Phys. Atom. Nucl. 77(10), 1203–1215 (2014)
- Lee, S.Y.: Accelerator Physics. World scientific publishing (2018)
- Myers, S., Bruning, O.: Challenges and Goals for Accelerators in the XXI Century. World Scientific (2016)
- Rumolo, G.: Beam Instabilities arXiv preprint arXiv:1601.05201 (2016)
- Hofmann, A.: Introduction to Beam Instabilities. (2005)
- Métral, E., et al.: Beam instabilities in hadron synchrotrons. IEEE. Trans. Nucl. Sci. 63(2), 1001–1050 (2016)
- Chao, A.W., Mess, K.H.: Handbook of Accelerator Physics and Engineering. World Scientific, (1998)
- Kheifets, S.A., Zotter, B.W.: Impedances and Wakes in High-Energy Particle Accelerators. World Scientific, (1998)
- Heifets, S.A., Kheifets, S.A.: Coupling impedance in modern accelerators. Rev. Mod. Phys. 63, 631–673 (1991)
- Palumbo, L., Vaccaro, V.G., Zobov, M.: Wake Fields and Impedance arXiv preprint physics/0309023 (2003)
- Panofsky, W., Wenzel, W.: Transverse deflection of charged particles in radiofrequency fields. Rev. Sci. Instrum. 27, 967 (1956)
- Gluckstern, R.L., vanZejts, J., Zotter, B.: Coupling impedance of beam pipes of general cross section. Phys. Rev. 47(1), 656–663 (1993)
- Niedermayer, U., Eidam, L., Boine-Frankenheim, O.: Analytic modelling, simulation and interpretation of broadband beam coupling impedance bench measurements. Nucl. Instrum. Methods. Phys. Res. Sect. A Accel. Spectrom. Detect. Assoc. Equip. 776, 129–143 (2015). <https://doi.org/10.1016/j.nima.2014.12.053>
- Kuehn, E.: A mode-matching method for solving field problems in waveguide and resonator circuits. Archiv fuer Elektronik und Uebertragungstechnik. 27, 511–518 (1973)
- Assante, D., et al.: Coupling impedance of a charge travelling in a drift tube. IEEE. Trans. Magn. 41(5), 1924–1927 (2005)
- Assante, D., Verolino, L.: Efficient evaluation of the longitudinal coupling impedance of a plane strip. Pro. Electromagn. Res. M. 26, 251–265 (2012)
- Assante, D., Verolino, L.: Model for the evaluation of an angular slot's coupling impedance. Symmetry. 11(5), 700 (2019)
- Vaccaro, V.G.: Coupling impedance measurements: an improved wire method, No. INFN-TC-94-023 SCAN-9502087 (1994)
- Hahn, H., Pedersen, F.: Coaxial wire measurements of the longitudinal coupling impedance, No. BNL-50870. Brookhaven National Lab., (1978)

22. Tsutsui, H.: On single wire technique for transverse coupling impedance measurement. No. SL-Note-2002-034-AP. CERN-SL-Note-2002-034-AP (2002)
23. Eswaran, K.: On the solutions of a class of dual integral equations occurring in diffraction problems. Proc. Roy. Soc. Lond. A429, 399–427 (1990)
24. Abramowitz, M., Stegun, I.: Handbook of Mathematical Functions. National Bureau of Standards, (1964)
25. Gradshteyn, I.S., Ryzhik, I.M.: Table of Integrals, Series, and Products, 7th ed. Academic Press, (2007)
26. Lewin, L.: Structural Properties of Polylogarithms. American Mathematical Society, Providence (1991)

APPENDIX A

ELECTROSTATIC FIELD OF A CHARGE IN A PIPE

In this appendix, we show how to calculate the scalar potential and the electric field of an idle charge placed in a perfectly conductive pipe. In order not to confuse the notation with the previous formulation, all the spatial and electrical quantities are primed, since this notation is used in the frame of the particle where all the charges are stationary.

The distance in cylindrical coordinates can be expanded as [28].

$$\frac{1}{\sqrt{r_1^2 + r_2^2 - 2r_1r_2 \cos(\varphi - \varphi_0) + (z - z_0)^2}} = \frac{1}{\pi} \sum_{m=-\infty}^{+\infty} e^{jm(\varphi - \varphi_0)} \int_{-\infty}^{\infty} I_m(\omega r_1) K_m(\omega r_2) e^{-j\omega(z - z_0)} d\omega \quad (47)$$

with $r_1 \leq r_2$.

Therefore, the electrostatic potential produced by a charge placed in $(r_q, \varphi_q, 0)$ in free space can be expressed as

$$V'_q = q \sum_{m=-\infty}^{+\infty} e^{jm(\varphi' - \varphi_q)} \int_{-\infty}^{\infty} G_m^q(r', r_q, \omega) e^{-j\omega z'} d\omega \quad (48)$$

where

$$G_m^q(r', r_q, \omega) = \frac{1}{4\pi^2 \epsilon_0} \begin{cases} K_m(\omega r') I_m(\omega r_q); & r' \geq r_q \\ K_m(\omega r_q) I_m(\omega r'); & r' \leq r_q \end{cases} \quad (49)$$

The charge inside the pipe induces on the pipe surface a charge density $\sigma'_p(r' = b, \varphi', z')$, producing a potential

$$V'_p = b \int_{-\infty}^{+\infty} \int_{-\pi}^{+\pi} \sigma'_p(\varphi'_0, z'_0) \sum_{m=-\infty}^{+\infty} e^{jm(\varphi' - \varphi_0)} \cdot \int_{-\infty}^{+\infty} G_m^q(r', b, \omega) e^{-j\omega(z' - z'_0)} d\omega d\varphi'_0 dz'_0 \quad (50)$$

The pipe being perfectly conductive corresponds to impose that the total scalar potential is constant. Since the potential of one arbitrary point can be fixed at zero, we choose

27. Kovetz, A.: Electromagnetic Theory. Oxford University Press (2000)
28. Jackson, J.D.: Classical Electrodynamics. Wiley, (1999)

How to cite this article: Assante, D., et al.: Coupling impedance of a PEC angular strip in a vacuum pipe. IET Microw. Antennas Propag. 15(10), 1347–1359 (2021). <https://doi.org/10.1049/mia2.12181>

such a condition on the pipe. Therefore, with some manipulations, we obtain

$$\int_{-\infty}^{+\infty} \int_{-\pi}^{+\pi} \sigma'_p(\varphi'_0, z'_0) \sum_{m=-\infty}^{+\infty} e^{jm(\varphi' - \varphi_0)} \cdot \int_{-\infty}^{+\infty} G_m^q(b, b, \omega) e^{-j\omega(z' - z'_0)} d\omega d\varphi'_0 dz'_0 = \quad (51)$$

$$= -\frac{q}{b} \sum_{m=-\infty}^{+\infty} e^{jm(\varphi' - \varphi_q)} \int_{-\infty}^{+\infty} G_m^q(b, r_q, \omega) e^{-j\omega z'} d\omega$$

for every φ', z' on the pipe.

Considering that

$$\int_{-\pi}^{+\pi} e^{jm\varphi'} e^{-jn\varphi'} d\varphi' = 2\pi \delta_{mn} \quad (52)$$

Then, with some manipulations, it is found that

$$\int_{-\infty}^{+\infty} \int_{-\pi}^{+\pi} \sigma'_p(\varphi'_0, z'_0) e^{j(\omega z'_0 - m\varphi'_0)} d\varphi'_0 dz'_0 = \quad (53)$$

$$= -\frac{q}{b} e^{-jm\varphi_q} \frac{G_m^q(b, r_q, \omega)}{G_m^q(b, b, \omega)}$$

This allows to express the induced charge density, with some manipulations, as a Fourier series:

$$\sigma'_p(\varphi', z') = -\frac{4\pi^2 q}{b} \sum_{m=0}^{+\infty} e^{jm(\varphi - \varphi_q)} \int_{-\infty}^{+\infty} \frac{I_m(\omega r_q)}{I_m(\omega b)} e^{-j\omega z'} d\omega \quad (54)$$

Therefore, Equation (50) can be rewritten as

$$V'_p = -q \sum_{m=-\infty}^{+\infty} e^{jm(\varphi' - \varphi_q)} \int_{-\infty}^{+\infty} G_m^q(r', b, \omega) e^{-j\omega z'} d\omega \quad (55)$$

being

$$G_m^p(r', r_q, \omega) = -\frac{1}{4\pi^2 \epsilon_0} \frac{I_m(\omega r_q)}{I_m(\omega b)} K_m(\omega b) I_m(\omega r') \quad (56)$$

Finally, the scalar potential of a charge in a pipe can be expressed as

$$V'_{qp} = q \sum_{m=-\infty}^{+\infty} e^{jm(\varphi'-\varphi_q)} \int_{-\infty}^{+\infty} G_m^{qp}(r', b, w) e^{-jwz'} d\tau \quad (57)$$

being

$$G_m^{qp}(r', r_q, w) = \frac{1}{4\pi^2 \epsilon_0} \begin{cases} K_m(wr') I_m(wr_q) - \frac{I_m(wr_q)}{I_m(wb)} K_m(wb) I_m(wr'); \\ r' \geq r_q \\ K_m(wr_q) I_m(wr') - \frac{I_m(wr_q)}{I_m(wb)} K_m(wb) I_m(wr'); \\ r' \leq r_q \end{cases} \quad (58)$$

Therefore, the three components of the electric field of a charge in a perfectly conductive pipe can be expressed as follows:

$$e'_{r,qp} = -q \sum_{m=-\infty}^{+\infty} e^{jm(\varphi'-\varphi_q)} \int_{-\infty}^{+\infty} \frac{\partial G_m^{qp}}{\partial r'}(r', r_q, w) e^{-jwz'} d\tau \quad (59)$$

$$e'_{\varphi,qp} = -\frac{j2q}{r'} \sum_{m=-\infty}^{+\infty} m e^{jm(\varphi'-\varphi_q)} \int_{-\infty}^{+\infty} G_m^{qp}(r', r_q, w) e^{-jwz'} d\tau \quad (60)$$

$$e'_{z,qp} = jq \sum_{m=-\infty}^{+\infty} e^{jm(\varphi'-\varphi_q)} \int_{-\infty}^{+\infty} w G_m^{qp}(r', r_q, w) e^{-jwz'} d\tau \quad (61)$$

APPENDIX B

RELATION WITH PREVIOUS WORKS

Some of the authors have already discussed in [19] the problem of a particle travelling parallel to an angular strip in the free space that is in the absence of the pipe. In this section, we show how the previous work can be considered a special case of the present formulation and the improvements in the present formulation.

In order to consider the angular strip in the free space in the present formulation, it is possible to consider the limit for $b \rightarrow \infty$. In such a limit, Equation (7) tends to Equation (49). Then, considering that

$$K_0\left(w\sqrt{r_1^2 + r_2^2 - 2r_1r_2\cos(\varphi - \varphi_0)}\right) = \sum_{m=-\infty}^{+\infty} e^{jm(\varphi-\varphi_0)} I_m(wr_1) K_m(wr_2) \quad (62)$$

with $r_1 \leq r_2$, it is easy to verify that Equation (13) is a generalisation of Equation (10) in [19].

However, the present work is not just a generalisation of [19]. In the previous study, the adopted project scheme did not benefit from the possible expansion of the potentials and fields in cylindrical harmonics. The expansion (16) is just replaced into the integral equation, which is directly projected on the same expansion basis. Instead, in this study, the adoption of the projection scheme based on Equation (17), allows to fully take advantage of the Neumann series expansion, leading to a more efficient and more accurate calculation of the coefficients of the linear system Equation (21). It is trivial to verify that in the actual formulation, in the case $b \rightarrow \infty$, adopting the same projection scheme of [19], the same expression of **A** and **b** would have been found.